Advanced Mechanical and Mechatronic Systems

Research Article
Volume 1(1), 2025, 29–51
https://doi.org/10.53623/amms.v1i1.675

Finite Element Analysis and Vibration Signal Processing Techniques To Determine the Frequency Response in Bridge Health Monitoring Study

Yogi Reza Ramadhan[1]*, Muhammad Nazri[2], Seno Adi Putra[3], Marina Riviani Rompas[1], Januar Panca Adi[1], Natalino Fonseca D. S. Guterres[4], Salustiano dos Reis Piedade[4]

[1]CV. Rekayasa Desain Manufaktur (REDESMA), Tembalang, Semarang, Indonesia
[2]Department of Electrical Engineering, Universiti Teknologi Brunei, Brunei Darussalam
[3]School of Industrial and System Engineering, Telkom University, Bandung, Indonesia
[4]Mechanical Engineering Department, Dili Institute of Teknology, Rua de Aimeti Laran, Aimutin Dili, Timor Leste

Correspondence: yogireza07@gmail.com

SUBMITTED: 2 May 2025; REVISED: 16 June 2025; ACCEPTED: 19 June 2025

ABSTRACT: Ensuring the structural integrity of large-scale bridges is critical worldwide, particularly in Indonesia. The integration of modern digital technologies significantly enhances this effort. A bridge health monitoring system is a vital tool for collecting data, allowing authorities to assess bridge conditions and refine inspection methods. Vibration responses measured using accelerometers, offer valuable insights into a bridge's structural health. However, the complexity of vibration signals requires advanced signal processing techniques to extract meaningful information. Empirical Mode Decomposition (EMD) and Wavelet Packet Decomposition (WPD) are two promising methods for analyzing such complex signals. Given the large scale of bridge structures and the limited number of sensors typically available, researchers often use Finite Element Analysis (FEA) to simulate and predict vibration responses. For example, a study on the Cisomang Bridge in Bandung, Indonesia, employed FEA to model the bridge's vibration characteristics. The first natural frequency identified was approximately 4.732 Hz, which served as a reference for further analysis. By integrating FEA models with advanced signal processing methods, the system aims to deliver reliable tools for monitoring and maintaining bridge health, thereby improving infrastructure safety and longevity.

KEYWORDS: Bridge health monitoring; EMD; FEA; structural integrity; vibration signal analysis; WPD

1. Introduction

In Southeast Asian countries, large-scale bridges had been built decades ago. Many of these bridges experienced wear and tear over time. Thus, to prolong their functionality, they definitely required maintenance and repair. There were several incidents of bridge-related disasters around the world, resulting in damage or even collapse. To improve the safety of both bridge users and the structures themselves, it was important to monitor the condition of these recently constructed bridges [1]. Solutions had been proposed through the use of bridge health monitoring systems. A bridge health monitoring system implemented structural health monitoring and inspection for bridges. Health monitoring for structures had evolved over time. A system capable of continuously monitoring and detecting damage in bridges could reduce the need for manual labor. More complex systems included data acquisition units that recorded and transmitted data offsite [2]. These systems often involved a large number of sensors, which could cost as much as, or even more than, the construction of the bridge itself. Various types of sensors contributed to such systems, including accelerometers, climatic sensors (such as temperature, wind speed and direction, humidity), displacement sensors, and load sensors [1]. Accelerometers measured the instantaneous velocity rate of a vibrating bridge at specific points. These measurements could be compared with earlier readings to detect deterioration or structural damage. Therefore, it was necessary to identify a more cost-effective approach to analyze the bridge data and extract useful information [3].

The aim of this research was to study the condition particularly the frequency response,of a bridge using FEA and vibration analysis, referred to here as a Bridge Health Monitoring System (BHMS), to notify or alert relevant authorities of potential structural issues. Upon examining the frequency response, this study also aimed to explore improved techniques and methods to provide an affordable and innovative solution for bridge monitoring. In recent years, ANSYS software emerged as a powerful tool for modeling and analyzing the behavior of bridge structures under varying conditions. The software provided a range of capabilities that enabled engineers to computationally model a bridge's physical structure as a set of smaller interconnected elements, each with specific properties and behaviors. This study used FEA to conduct simulation studies on the structural integrity of bridges. Based on a Computer-Aided Drawing (CAD) model with detailed dimensions and materials, and an estimated load applied to the bridge, vibration analysis within the FEA software predicted the bridge's frequency response.

2. Materials and Methods

2.1. Vibration experiment and data processing.

2.1.1. Raw vibration data acquisition.

Raw vibration data was collected using accelerometer sensors mounted on the bridge structure. These sensors recorded the vibration responses of the bridge as vehicles passed over it, generating signal data that reflected the bridge's dynamic behavior. The data, typically in the form of time-domain signals, contained detailed information, including fluctuations resulting from varying vehicle loads and environmental conditions. The vibration data acquisition is presented in Figure 1.

2.1.2. Pre-processing of data.

The raw vibration signal needs to be pre-processed prior to the data analysis. These steps include: Filtering to remove unwanted noise or interference from the signal using a low-pass or high-pass filter as per the needs of the analysis and normalization to adjust the amplitude of the signal to ensure consistency in subsequent analysis.

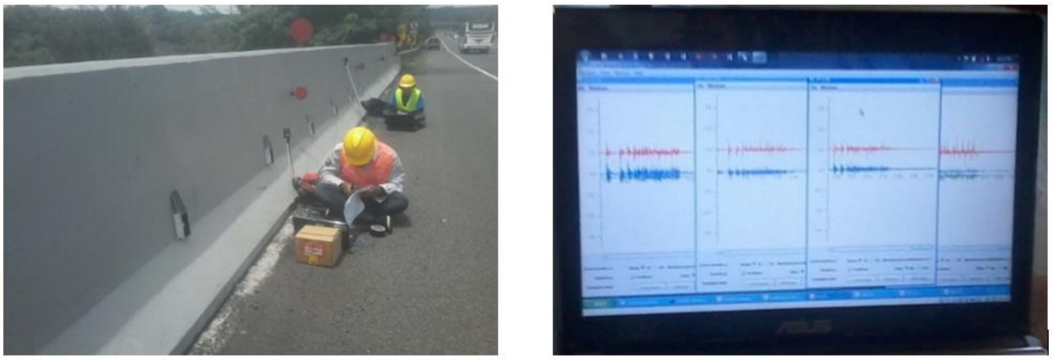
(a) (b)

Figure 1. (a) Vibration signal acquistion using accelerometer sensor attached on the side of the Cisomang bridge; (b). Vibration signal view from the DAQ software.

2.1.3. Signal processing (signal decomposition)

After the signal is pre-processor, the next step is the decomposition of the signal. The methods commonly used in this study are:

– Empirical Mode Decomposition (EMD): Breaks down complex signals into multiple IMFs. This process helps keep the information in a simpler and more focused form, making it easier to recognize patterns and features on the signal.
– Wavelet Packet Decomposition (WPD): Breaks down signals into approximation coefficients (A) and detail coefficients (D). WPD allows for multi-resolution analysis, which identifies frequency components at various scales.

2.1.4. Analysis and interpretation.

The extracted features are then analyzed to obtain more information regarding the condition of the bridge. For example, identifying whether there are certain patterns that indicate possible breakdowns or by comparing the vibration responses of different types of vehicles.

2.2. Finte element method (FEM).

Bridges played a crucial role in ensuring safe and efficient transportation, and the use of advanced technology was essential for designing and maintaining these vital structures. ANSYS software served as a powerful tool for modeling and analyzing the behavior of bridge structures under various conditions. This software offered a range of tools and capabilities that enabled engineers to model the physical structure of a bridge as a collection of interconnected smaller elements, each with its own properties and behaviors.

By dividing the structure into smaller elements such as beams, columns, and frames, engineers applied FEA techniques to simulate the bridge's behavior under specific conditions. To analyze the structural response to moving vehicle loads, suitable analysis methods such as transient structural analysis were employed. This technique allowed for the simulation of time-dependent loads and accurately modeled the bridge's dynamic response to vehicle movement.

Signal processing techniques, including Fourier analysis, were used to identify the natural frequencies of the bridge. These frequencies represented the points at which the structure exhibited the greatest vibration in response to external loads and were critical in identifying potential sources of fatigue or structural failure.

A typical bridge with a single beam and support columns at either end, when excited at its first natural frequency referred to as the first fundamental mode, exhibited a curvature at the midpoint of the beam. At the second natural frequency, or second fundamental mode, two distinct curvature points could be observed. At the third natural frequency, the structure often demonstrated a twisting motion. Through analysis of mode shapes and natural frequencies, engineers gained deeper insights into the bridge's dynamic behavior and were able to identify areas susceptible to failure or degradation.

Such information was essential for designing safe and durable bridges capable of withstanding a variety of operational loads and environmental conditions. Engineers could then develop appropriate safety measures to mitigate risks and extend the lifespan of these critical infrastructures. Figure 2 presented the research methodology flow chart, outlining the two main processes used in this study: FEA and vibration analysis. A computational finite element model (FEM) was developed using assigned material properties. The model incorporated element meshing and connectivity based on the defined boundary conditions. A static structural analysis was then conducted, and the resulting output provided the frequency response of the bridge, indicating the dominant or calculated natural frequency.

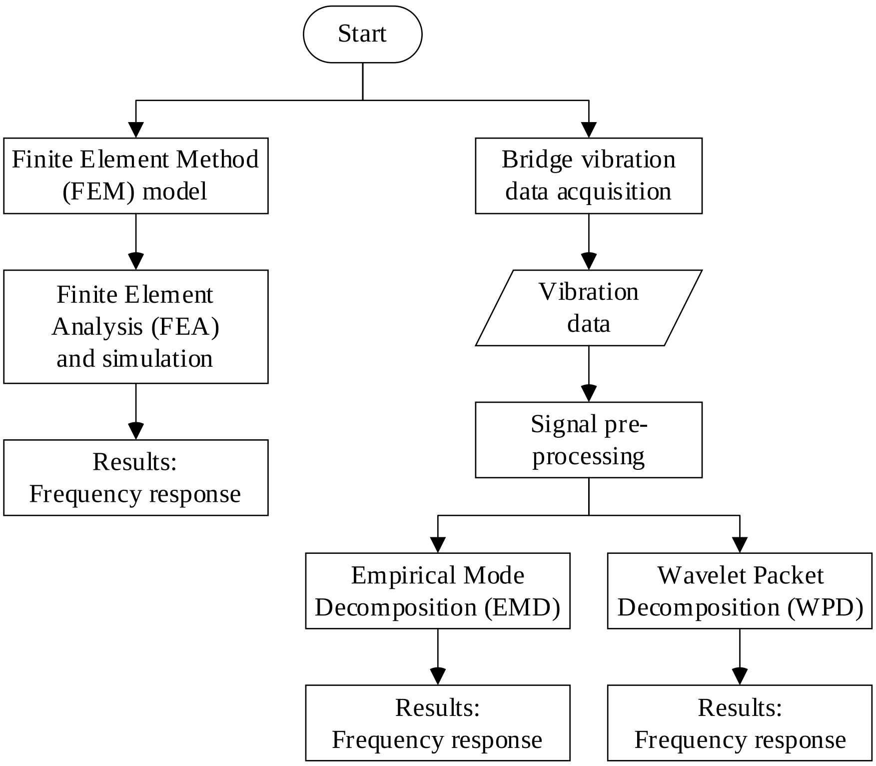

Figure 2. Research methodology flow chart.

A flow chart of both simulation and experiment studies is presented in Figure 2. It is showed in Figure 2 that that two methods, namely EMD and WPD, were used to decompose the vibration signal. The decomposed signals were further processed using the Fast Fourier Transform (FFT) to identify any relevant or significant frequency content related to the FEM results. The outcomes of these techniques revealed the frequency response of the bridge. These results were then compared with the computational results. The bridge structure was modeled in ANSYS; therefore, accurate dimensions and material properties of the bridge components were required to ensure the highest possible precision. A concrete cross-section reinforcement strength of 4000 psi, equivalent to approximately 27.6 MPa, was used, which met the requirements of the American Society for Testing and Materials (ASTM). Table 1 presents the material properties of the bridge components.

Table 1. Material properties of the underpass bridge components.

Element/ Components	Material	Property			
		Density (kg/m^3)	Elasticity (Mpa)	Quality (Mpa)	Poisson's Ratio
Girder beam	Concrete	2400	30,277	41.5	0.2
Concrete plate	Concrete	2400	25,741	30	0.2
Tendon	Steel	7850	200,000	1860	

2.3 EMD.

The selected time-frequency representation method for this study was EMD [4], which has been proven effective for non-stationary and non-linear signal applications, as demonstrated by Braun and Feldman [5]. The EMD method operated based on an enveloping technique known as the Hilbert-Huang Transform, which decomposed raw vibration signals into several components ranging from high to low frequencies. These decomposed signals were referred to as IMFs. An IMF is a signal component derived from the decomposition of the original signal into multiple frequency-based modes. Each IMF possesses a unique frequency and amplitude, representing the vibrational characteristics of the analyzed structure, such as a bridge. The IMFs were arranged from high to low frequency. In condition monitoring of rolling element bearings, EMD has been used to reveal frequency content by decomposing the original vibration signal into IMFs. Preliminary studies on condition monitoring [6–9] employed the original EMD approach [4] to analyze non-stationary slew bearing data. Due to its ability to isolate low-frequency components after reducing high-frequency noise, EMD shows potential for application in bridge monitoring.

EMD is a valuable technique for simplifying complex datasets into a series of IMFs through Hilbert spectral analysis. It has been successfully applied in bridge damage detection [10, 11], in identifying stiffness variations during vehicle–bridge interaction [10], and in determining bridge frequency responses from passing vehicles [11]. The core aim of EMD is to empirically decompose intrinsic oscillation modes based on their time-domain characteristics. During the decomposition, extreme oscillations without zero-crossings are excluded through a process known as shifting. As a result, the EMD algorithm isolates oscillatory components in a highly localized time domain, enabling the separation of overlapping signals into distinct, interpretable parts.

2.4. WPD.

The wavelet transform was an effective technique for analyzing non-stationary and transient signals [12]. It utilized wavelets as basis functions instead of sinusoidal functions by introducing a scale variable in addition to the time variable, thereby capturing transitions across different frequency components. Similar to EMD, wavelet decomposition broke down the original signal into multiple components based on the selected wavelet function [13].

The WPD method was a variant of wavelet decomposition designed to analyze signal behavior across a broader frequency spectrum, enabling the examination of the most relevant signal features. This approach involved a recursive filtering process that reduced time resolution while improving frequency resolution. In essence, wavelet decomposition separated the input signal into two sub-band components: (1) the 'approximate coefficient' (A), resulting from the input signal passing through a low-pass filter, and (2) the 'detail coefficient' (D), generated by passing the signal through a high-pass filter. The detail coefficients captured high-frequency information, whereas the low-frequency content held the most critical structural information. As a result, the approximate coefficients were further processed in a layered wavelet system for deeper decomposition [14].

At each approximation level, these coefficients were further divided into new approximation and detail coefficients, enabling continued decomposition. This recursive process could generate up to $2(2^{(n-1)})$ distinct encoding paths, forming the basis of the WPD method. In advanced applications, both the approximation and detail coefficients were repeatedly decomposed, constructing a complete structure suitable for comprehensive signal analysis. Selecting an appropriate decomposition strategy for a given signal required careful consideration of the entropy criterion, which determined how information was distributed across the nodes in the decomposition tree. The wavelet method encompassed various families, including Biorthogonal, Coiflets, Symlets, Daubechies, and Haar wavelets [15].

3. Results and Discussion

3.1. FEM result and analysis.

In FEM bridge simulation, several boundary conditions are determined as follows:

a. Material type of H-Beam structure: low alloy steel, 4140 (normalized).
b. Material type of bridge: concrete
c. The different forces applied on the bridge: 160kN (16315kg)
d. Frequency range: 0-38Hz

In this simulation, the parameters used for the bridge components is shown in a screenshoot of the ANSYS paremater properties presented in Figures 3 and 4. A low alloy steel, 4140 (normalizes) and concrete modeling parameters is presented in Figures 3 and 4, respectively.

Properties of Outline Row 4: Structural Steel

	A	B	C
1	Property	Value	Unit
2	Material Field Variables	Table	
3	Density	7850	kg m^-3
4	Isotropic Secant Coefficient of Thermal Expansion		
5	Coefficient of Thermal Expansion	1.2E-05	C^-1
6	Isotropic Elasticity		
7	Derive from	Young's ...	
8	Young's Modulus	2E+11	Pa
9	Poisson's Ratio	0.3	
10	Bulk Modulus	1.6667E+11	Pa
11	Shear Modulus	7.6923E+10	Pa

Figure 3. Parameters used in low alloy steel, 4140 (normalized).

Properties of Outline Row 4: Concrete			
	A	B	
1	Property	Value	
2	Material Field Variables	Table	
3	Density	2300	kg m^-3
4	Isotropic Secant Coefficient of Thermal Expansion		
5	Coefficient of Thermal Expansion	1.4E-05	C^-1
6	Isotropic Elasticity		
7	Derive from	Young's ...	
8	Young's Modulus	30000	MPa
9	Poisson's Ratio	0.18	
10	Bulk Modulus	1.5625E+10	Pa
11	Shear Modulus	1.2712E+10	Pa
12	Tensile Yield Strength	0	Pa
13	Compressive Yield Strength	0	Pa
14	Tensile Ultimate Strength	5	MPa
15	Compressive Ultimate Strength	41	MPa

Figure 4. Parameters used in the concrete.

Figure 5 shows the location of the 160 kN static force applied at the center of the 60-meter-long bridge. This location was selected because the accelerometer was installed at the midpoint of the bridge. As the vehicle passed over the bridge, this position received the load from the vehicle.

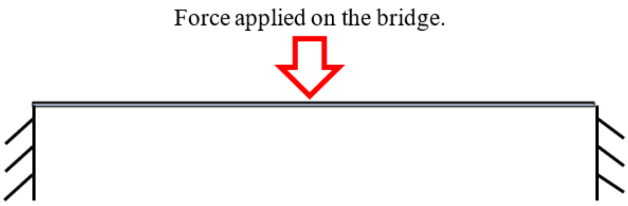

Figure 5. Position of force applied on the bridge.

The simulation results showed that when a 160 kN force was applied at the center of the bridge, the bridge vibrated across a range of frequencies, and at 4.732 Hz, it deformed the most, with a maximum amplitude of 14.228 mm. Figure 6 shows the maximum deformation (in red) of the bridge at 4.732 Hz.

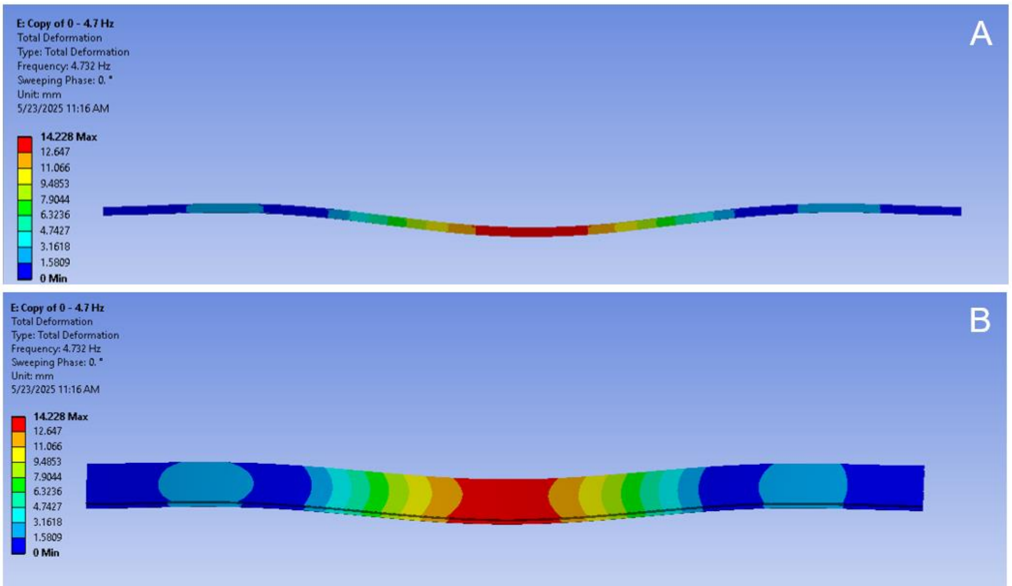

Figure 6. Deformation (mm) at the 4.732 Hz frequency: (A) side view; (B) 3D view.

The computed deformation data were extracted, and a graph showing the peak deformations is presented in Figure 7. The graph indicates two peak frequencies, 4.732 Hz and 16.02 Hz, with corresponding deformations of 14.228 mm and 0.978 mm, respectively. These deformation values remained below the allowable limits. Once the force was removed, the bridge returned to its original shape, indicating that the deformation was elastic.

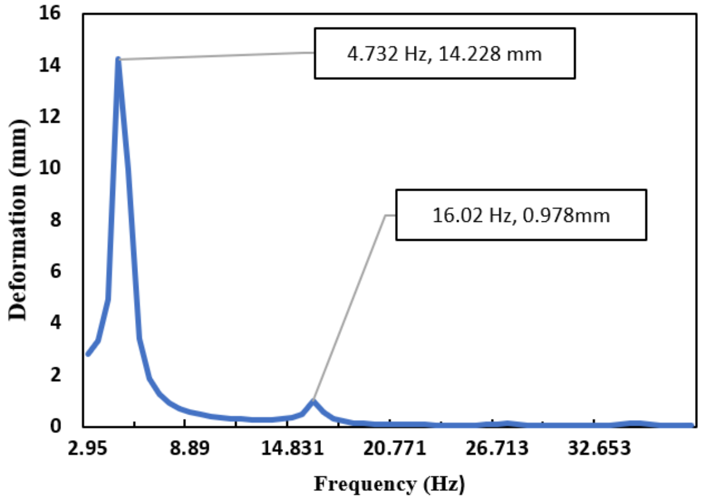

Figure 7. Deformation (mm) of the bridge at a range of frequency (Hz).

3.2. Vibration signal.

Vibration signals generated as five different types of vehicles passed over the bridge were recorded using a tri-axial accelerometer, as illustrated in Figure 8. Example vibration signals for each vehicle type are presented in Figure 9.

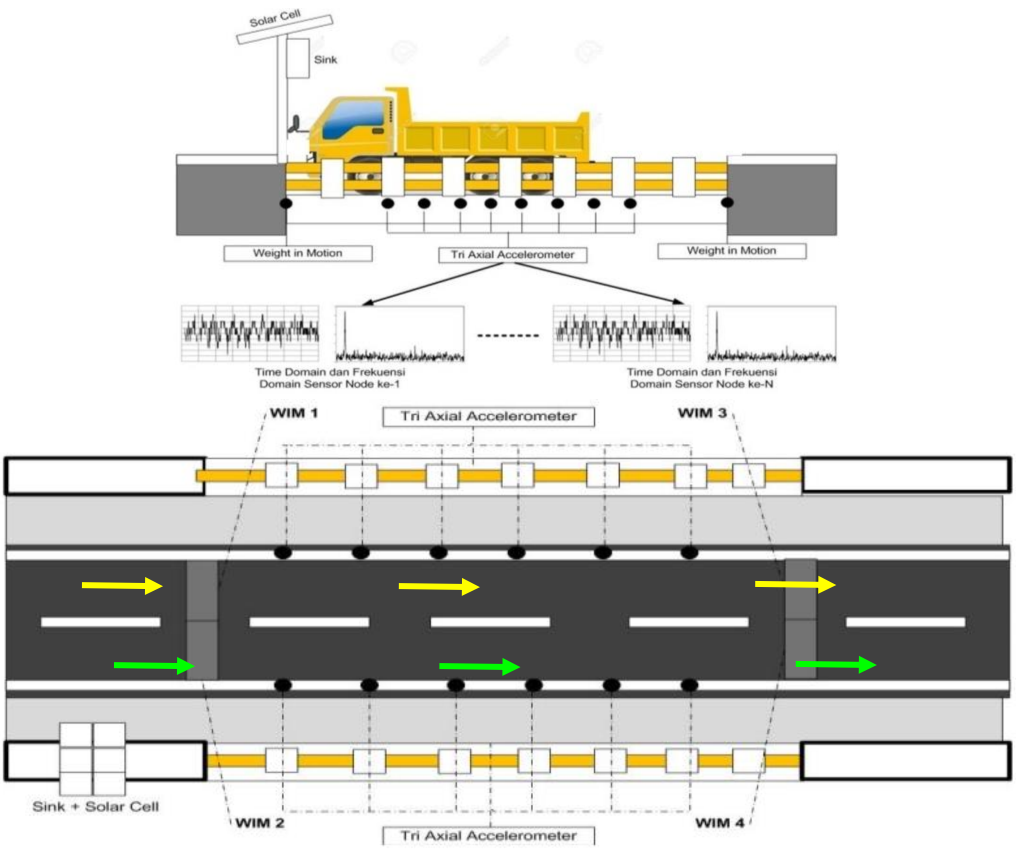

Figure 8. Placement of the bridge sensing system.

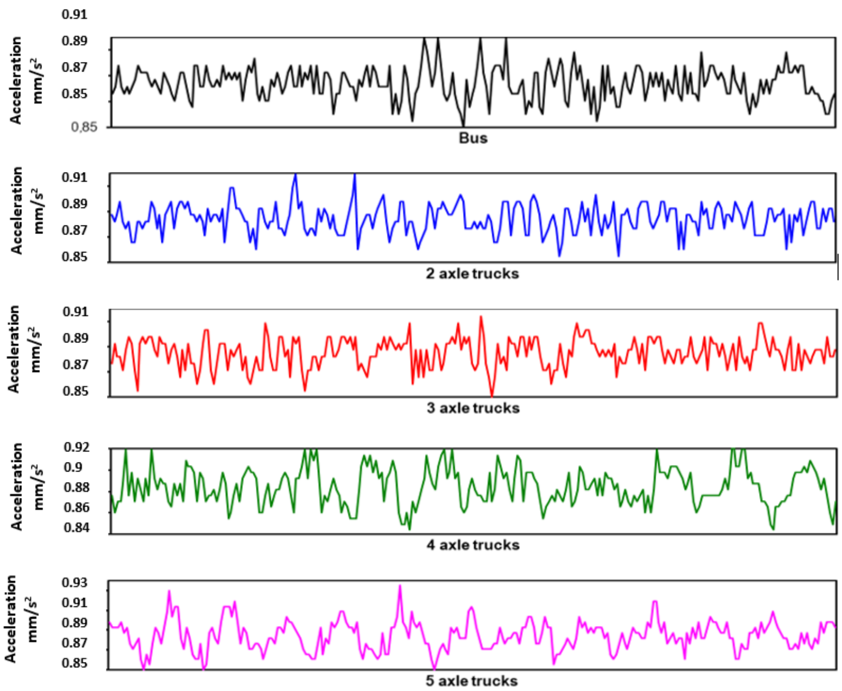

Figure 9. Raw signal from accelerometer sensor readings due to passing vehicles.

3.3. EMD results.

3.3.1. EMD result of the vibration signal when the bus passes through the bridge.

When the bus passed over the bridge in the left lane, the Weight-In-Motion (WIM) 1 sensor detected the approaching vehicle and activated the accelerometer node, while WIM 2 confirmed the vehicle type. The resulting vibration signals were decomposed into four IMFs, as presented in Figure 10.

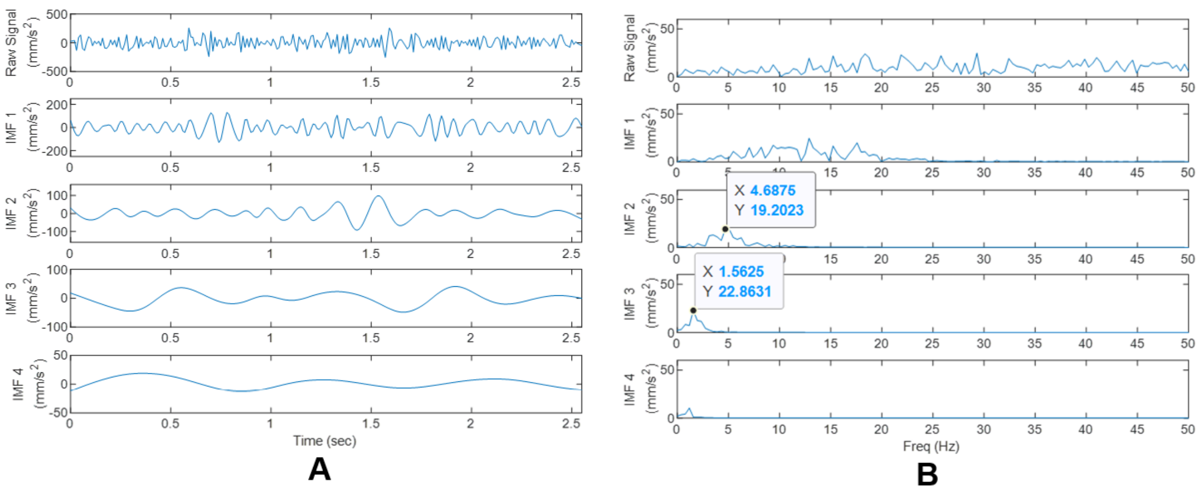

Figure 10. EMD decomposition results in vibrations when the bus over the bridge in (A) time and (B) frequency domain.

The raw vibration signal, shown in Figure 10A under 'Raw Signal', was decomposed using the EMD method to obtain IMF 1, 2, 3, and 4, as also presented in Figure 10A. The frequency content of each IMF signal was calculated using the FFT, as shown in Figure 10B. Based on the observation, IMF 2 was identified as the most relevant. The FFT of IMF 2 showed a dominant frequency of 4.687 Hz (rounded up to 4.688 Hz) with an amplitude of 19.202

mm/s². Additionally, IMF 3 exhibited a frequency of 1.562 Hz with a higher amplitude of 22.863 mm/s² compared to IMF 2.

3.3.2. EMD result of the vibration signal when the two-axles truck passes through the bridge.

The four IMFs of raw vibration signal when a two-axle truck passes through the bridge are presented in Figure 11. The four IMFs were processed in the FFT to calculate the frequency content as presented in Figure 11(b). Similar to Figure 10(b), Figure 11(b) shows a detection of 4.688 Hz dominant frequency with amplitude of 33.074 mm/s^2. This frequency is close to first fundamental frequency of the FEA result shows in Figure 7 i.e. 4.732 Hz. In addition, IMF 3 shows the frequency is 1.953 Hz with a vibration amplitude of 18.969 mm/s^2.

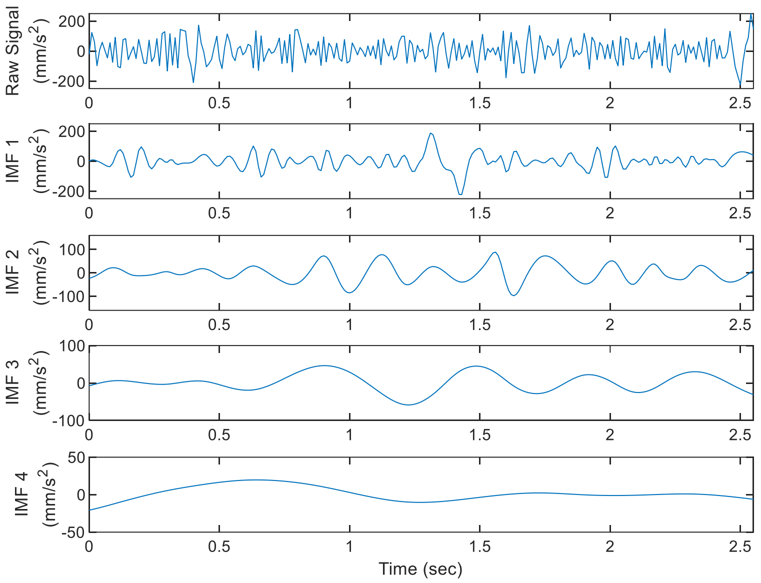

(a)

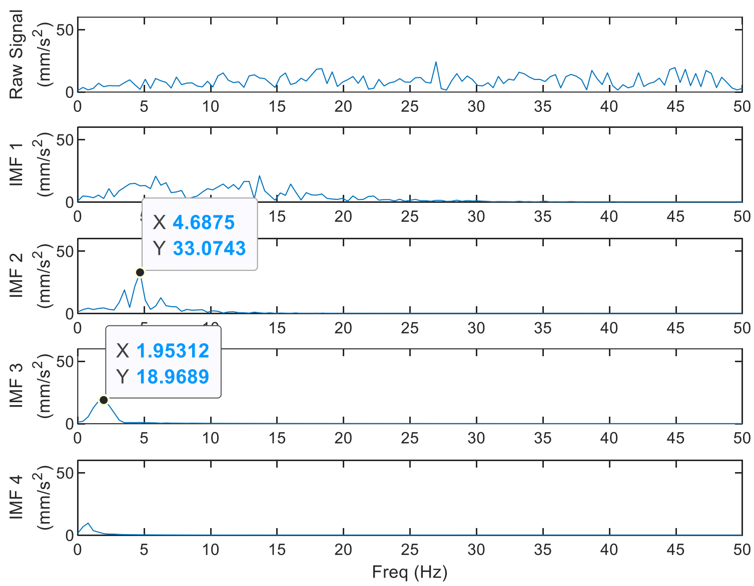

(b)

Figure 11. EMD decomposition results in vibrations when two axles truck over the bridge in (a) time and (b) frequency domain.

3.3.3. EMD result of the vibration signal when the three-axles truck passes through the bridge

The vibration signal when the three-axles truck passes trough the bridge and its four IMFs are is presented in Figure 12(a). As shown in Figure 12(b), frequency of 4.688 Hz is also obviously appeared with higher amplitude of 64.736 mm/s^2 compared to the previouse vehicle types. This indiciate that the mass of the vehicle when passes through the bridge is also affected to the frequency of the vibration signal.

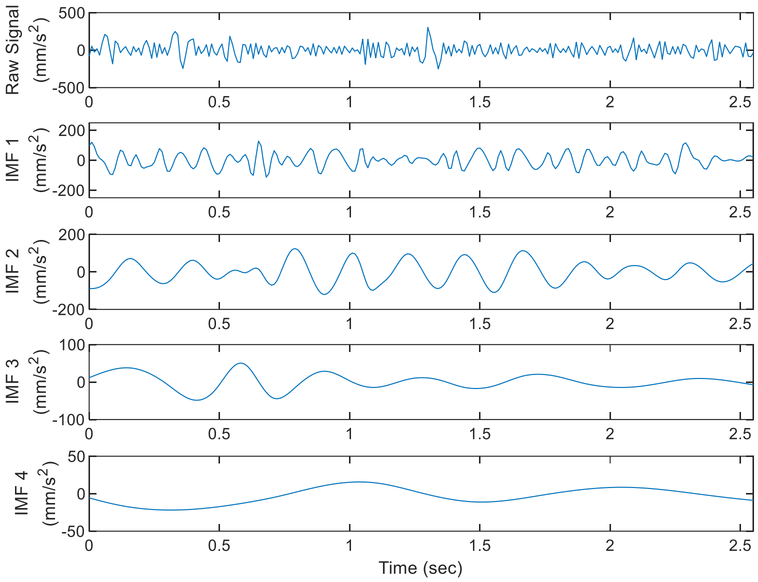

(a)

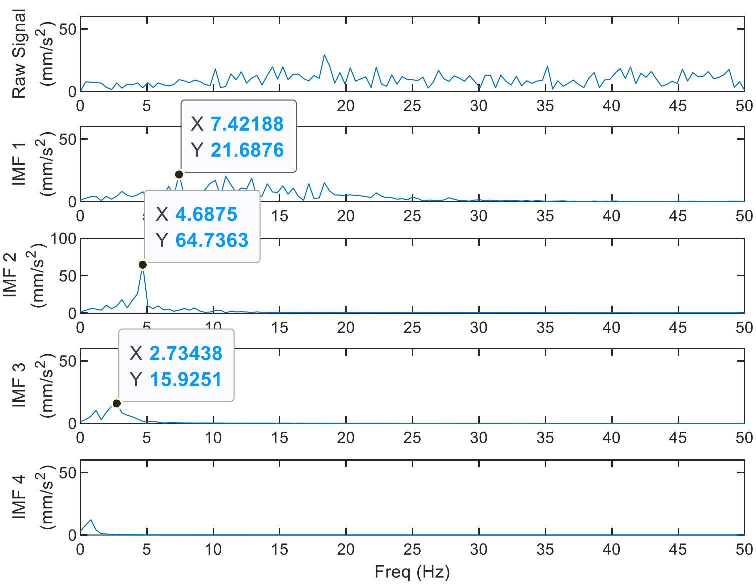

(b)

Figure 12. EMD decomposition results in vibrations when three axles truck over the bridge in (a) time and (b) frequency domain.

3.3.4. EMD result of the vibration signal when the four-axles truck passes through the bridge.

Similar to Figures 10(a), 11(a), and 12(a), Figure 13(a) shows the raw signal and IMFs of the decomposition results in time-domain. The IMFs were then processed in FFT to calculate the frequecy contentn. Focusing on the FFT of the IMF 2 as shown in Figure 13(b); the frequency content o 4.68 Hz has increased amplitude of 76.2 mm/s^2 compared to the other vehicle types in previous sections.

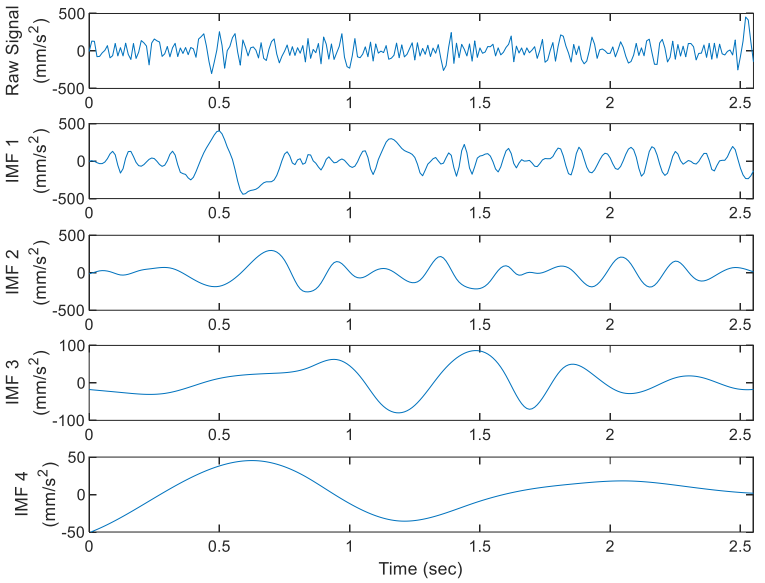

(a)

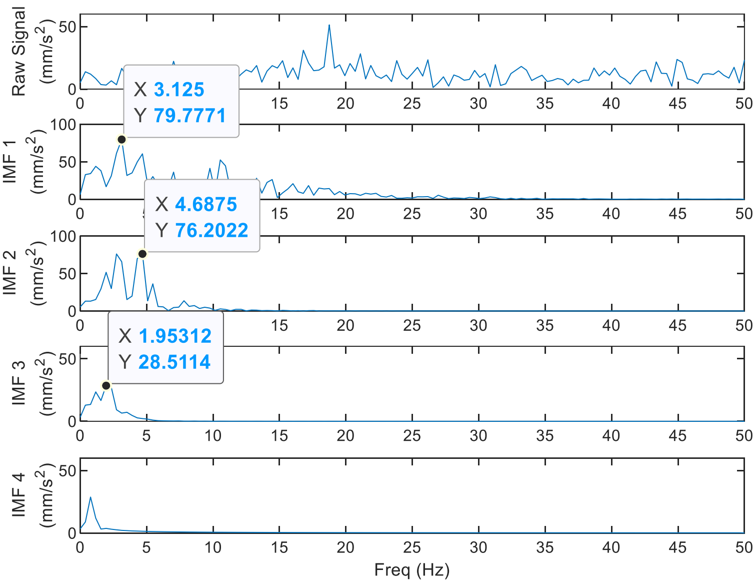

(b)

Figure 13. EMD decomposition results in vibrations when four axles truck over the bridge in (a) time and (b) frequency domain.

3.3.5. EMD result of the vibration signal when the five-axles truck passes through the bridge.

Figure 14(a) shows the raw signal and the IMFs of EMD. According to the FFT of the IMf 2 as presented in Figure 14(b), it support the hypothesis that the EMD method is one of potential methods to reval the fundamental or deformatin frequency of the bridge when different type of vehicles passes through the Cisomang bridge. As shown in Figure 14(b), a frequency of 4.6875 Hz is appeared with highest amplitude of 61.8756 mm/s^2 compare to other four types of vehicles.

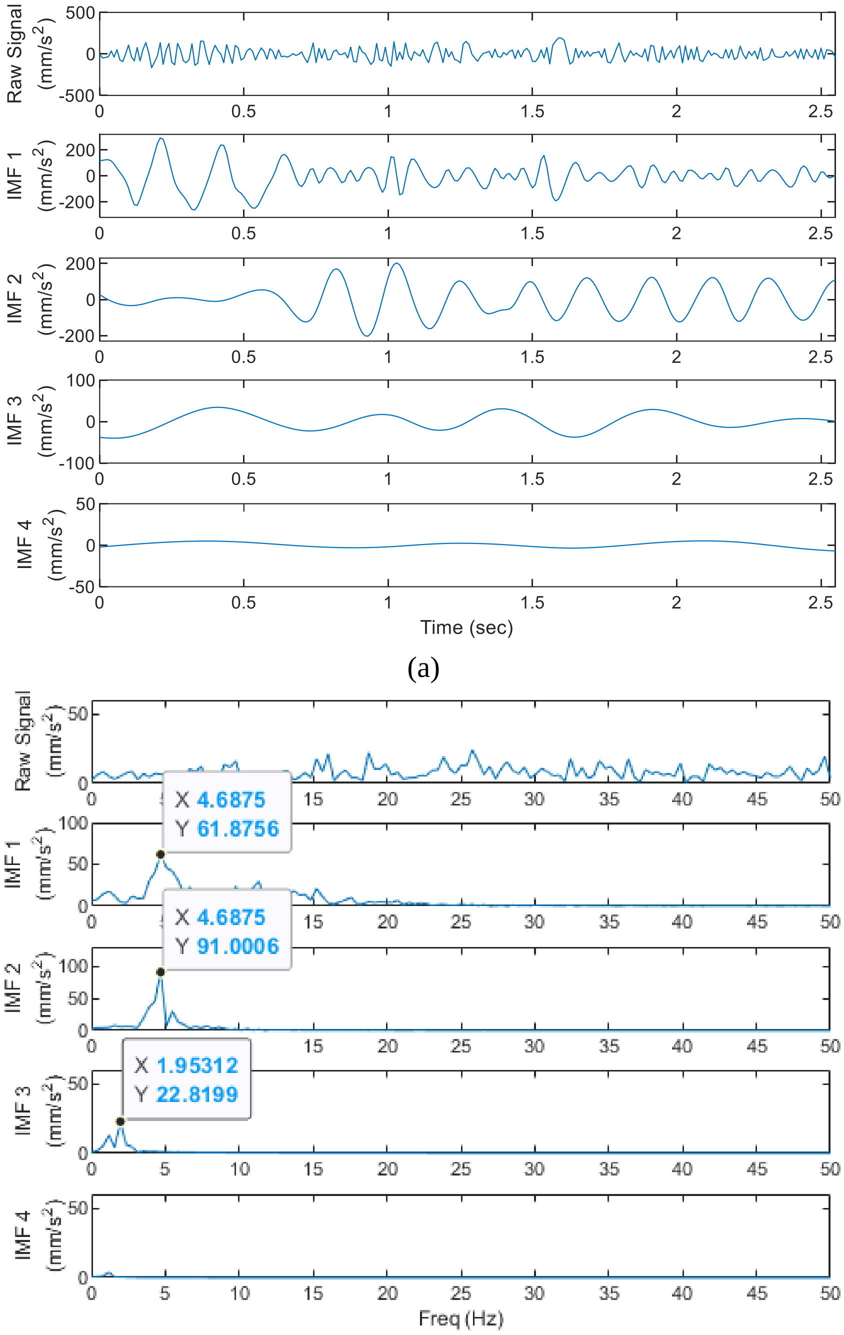

(b)

Figure 14. EMD decomposition results in vibrations when five axles truck over the bridge in (a) time and (b) frequency domain.

3.4 WPD results.

3.4.1. WPD result of the vibration signal when the bus passes through the bridge.

The vibration signal when the bus passes through the bridge was decomposed into four 'Detail coefficients', D1-D4 as shown in Figure 15(a). Please note that this paper did not present result of the 'Approximate coefficient' of the WPD method. The D1-D4 signals were then processed in FFT to calculated the frequency content. The result is presented in Figure 15(b). Our focus in on the D3 and D4 which shows a frequency of 4.688 Hz with an amplitude of 12.093 mm/s² and 9.471 mm/s². This frequency content is similar to the one obtained using the EMD method. In addition, this frequency is also close to the fundamental frequency of the FEA analysis result.

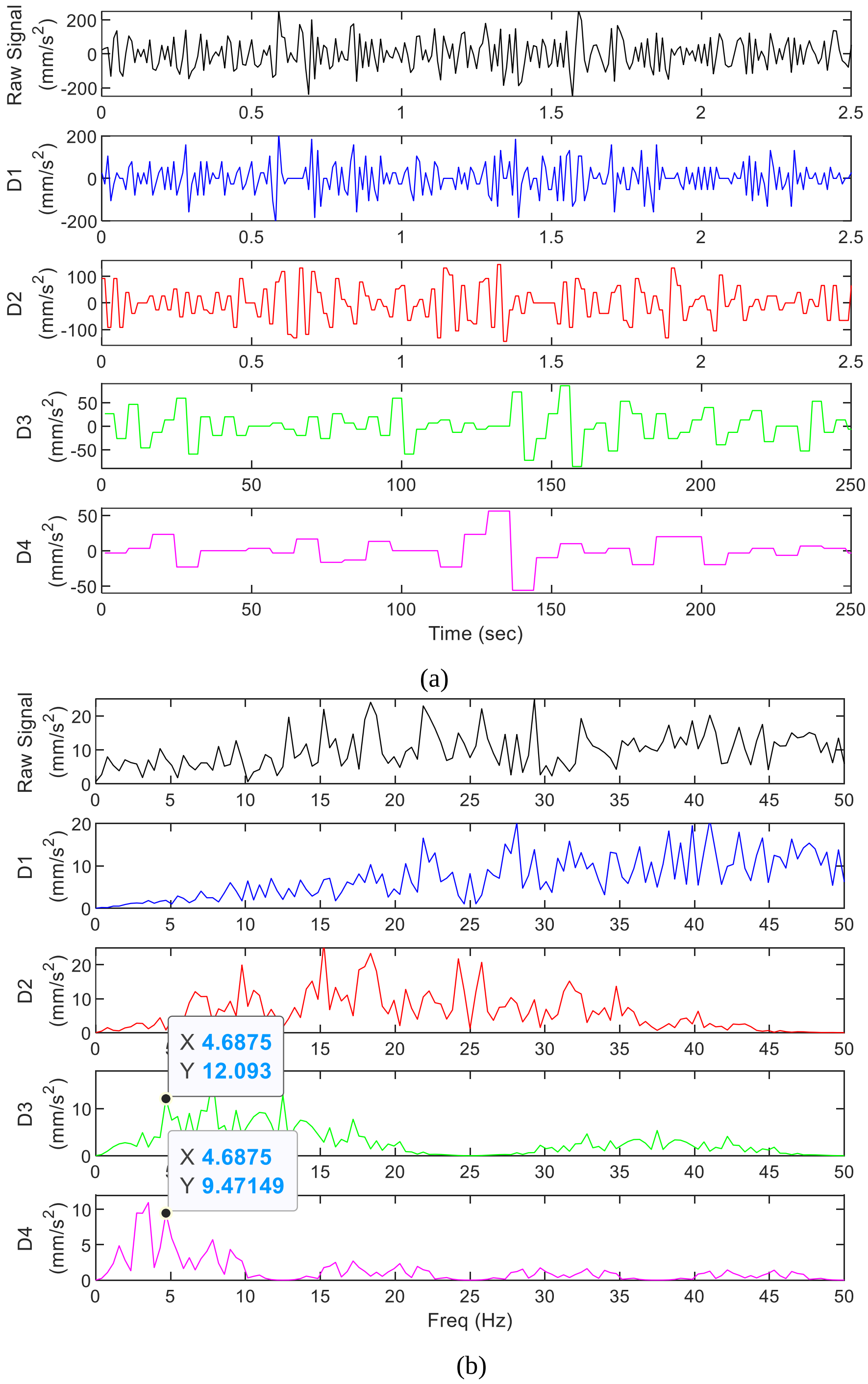

Figure 15. (a) Signal decomposition in time and (b) frequency domains for bus vehicle excitations.

3.4.2. WPD result of the vibration signal when the two-axles truck passes through the bridge.

Figure 16 shows the WPD decomposition signals in time (Figure 16(a)) and frequency (Figure 16(b)) domains of the bridge's vibration caused by excitation from a two-axles truck. An interesting result is shown in Figure 16(b) as the D2, D3, and D4 shows a fundamental frequency of 4.688 Hz with an amplitude of 7.632 mm/s², 11.856 mm/s², and 21.037 mm/s², respectively. This result indicates that the WPD method is more effective method to reveal the fundamental frequency when a certain vehicle passes through the bridge compare to EMD.

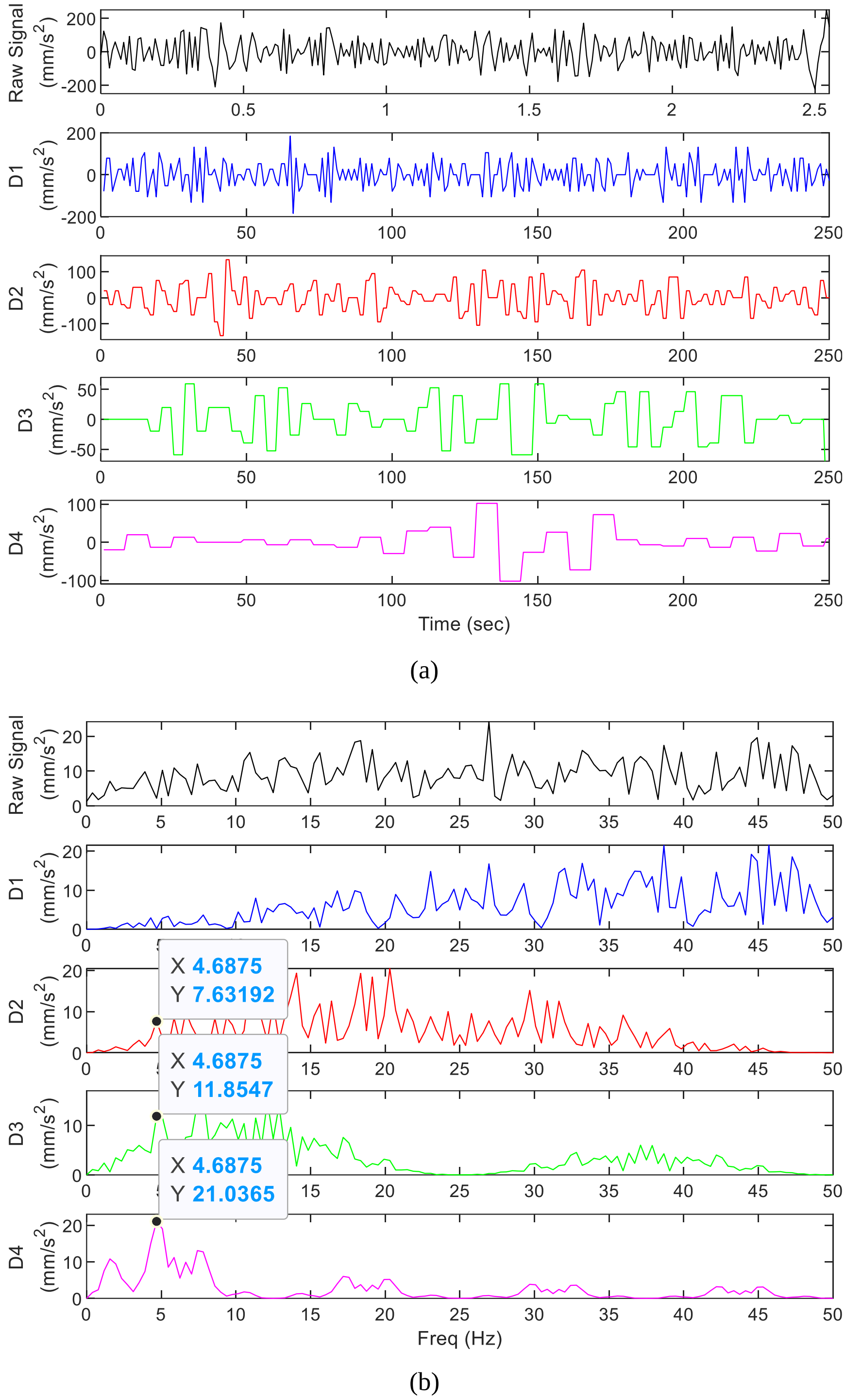

Figure 16. (a) Signal decomposition in time and (b) frequency domains for two-axles truck vehicle excitations.

3.4.3. WPD result of the vibration signal when the three-axles truck passes through the bridge.

The vibration signal when the bus passes through the bridge was decomposed into four ‘Detail coefficients’, D1-D4 as shown in Figure 17(a). Similar to the result obtained in Section 3.4.2 that the FFT of D2, D3, and D4 of the WPD result presented in Figure 17(b) shows the fundamental frequency of 4.688 Hz. The amplitude of this dominant frequency is higher than the result of the two-axles truck when passes through the bridge of 8.056 mm/s², 22.8 mm/s², and 38.823 mm/s², respectively. This indicates a consistency of the WPD method in decomposing the raw vibration signal that is when the weight is increase the amplitude also increased.

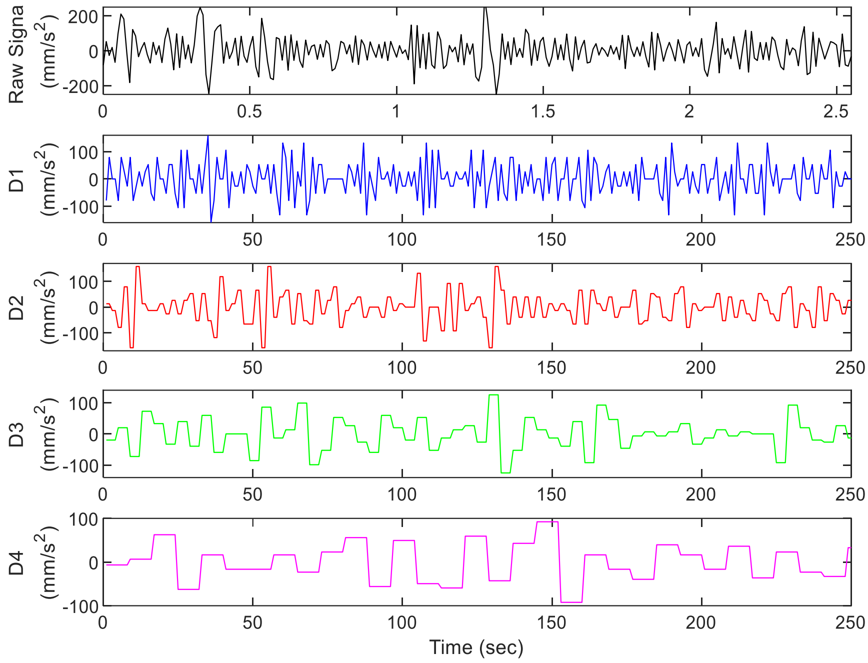

(a)

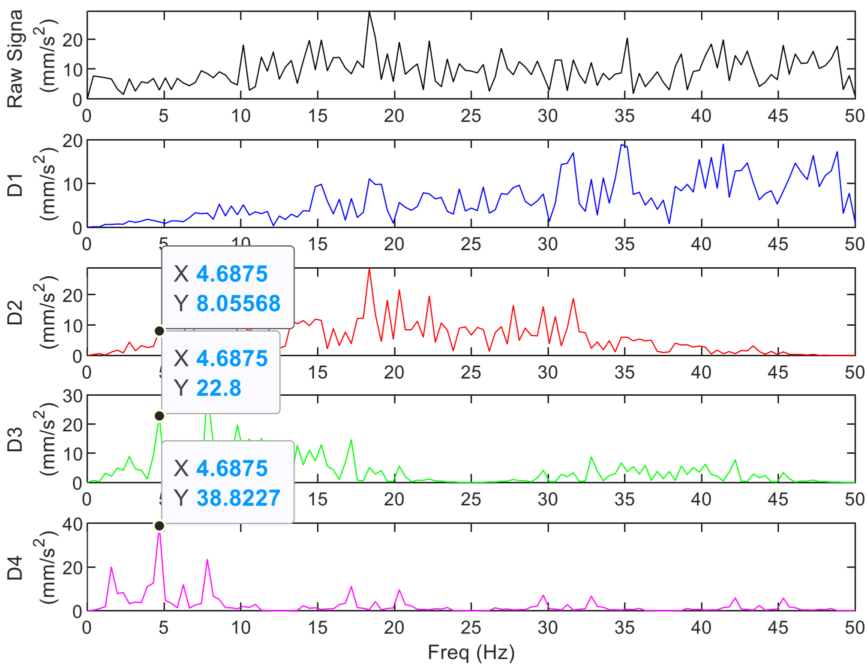

(b)

Figure 17. (a) Signal decomposition in time and (b) frequency domains for three-axles truck vehicle excitations.

3.4.4. WPD result of the vibration signal when the four-axles truck passes through the bridge.

When the four-axles truck passes through the bridge, the vibration signal is acquired and presented in the first row of Figure 18(a). Figure 18(a) also shows a detail coefficient of WPD and Figure 18(b) is the FFT of the associated detail signals. The FFT results in Figure 18(b) show that D1-D4 of WPD revealed the fundamental frequency of 4.688 Hz. The amplitudes of the D2 to D4 signals also increased significantly to 15.362 mm/s², 34.592 mm/s², and 69.931 mm/s², respectively, compared to those recorded from the previous vehicle types. This supports the analysis that the vehicle's weight has a significant impact on both the fundamental frequency and the resulting deformation. These results can be further utilized for effective bridge condition monitoring.

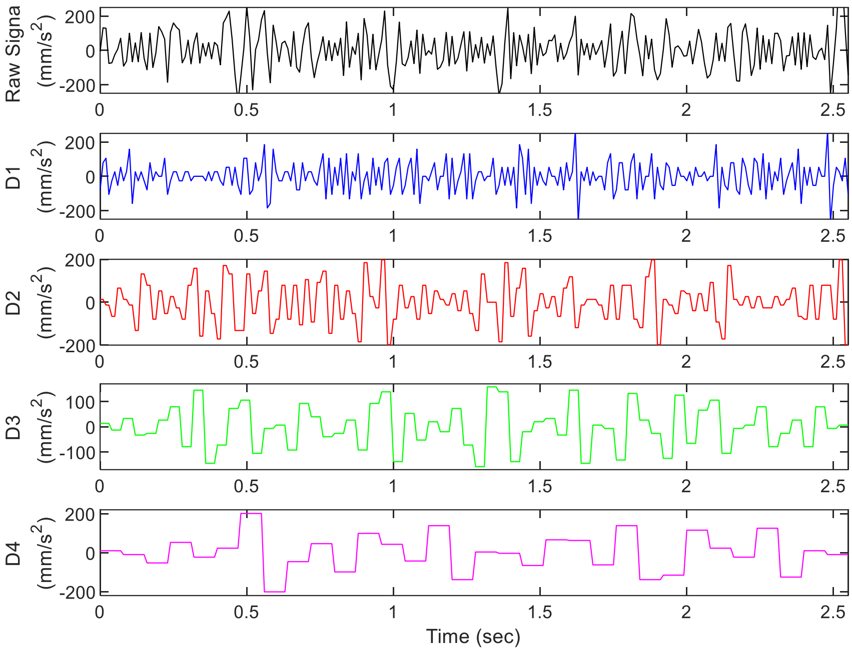

(a)

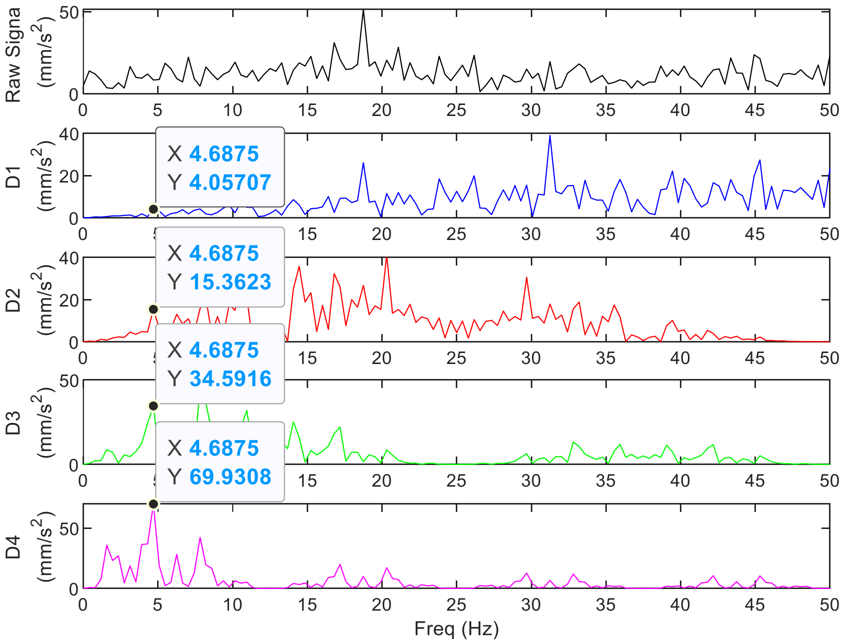

(b)

Figure 18. (a) Signal decomposition in time and (b) frequency domains for four-axles truck vehicle excitations.

3.4.5. WPD result of the vibration signal when the five-axles truck passes through the bridge.

The vibration signal of the five-axles truck passes through the bridge is shown Figure 19(a). Similar to the result presented in Figure 18(b), the FFT of D1-D4 decomposed signals in Figure 19(b) show the consistency result which revealed the fundamental frequency of 4.688 Hz. However, the amplitude of D1 and D2 signals was decreased to 2.461 mm/s² and 10.296 mm/s², respectively compared to the four-axles truck vibration analysis result. In contrast, the amplitude of D3 and D4 signals was increased to 42.808 mm/s² and 73.308 mm/s², respectively compared to the vibration signal of four-axles truck result when passes through the bridge.

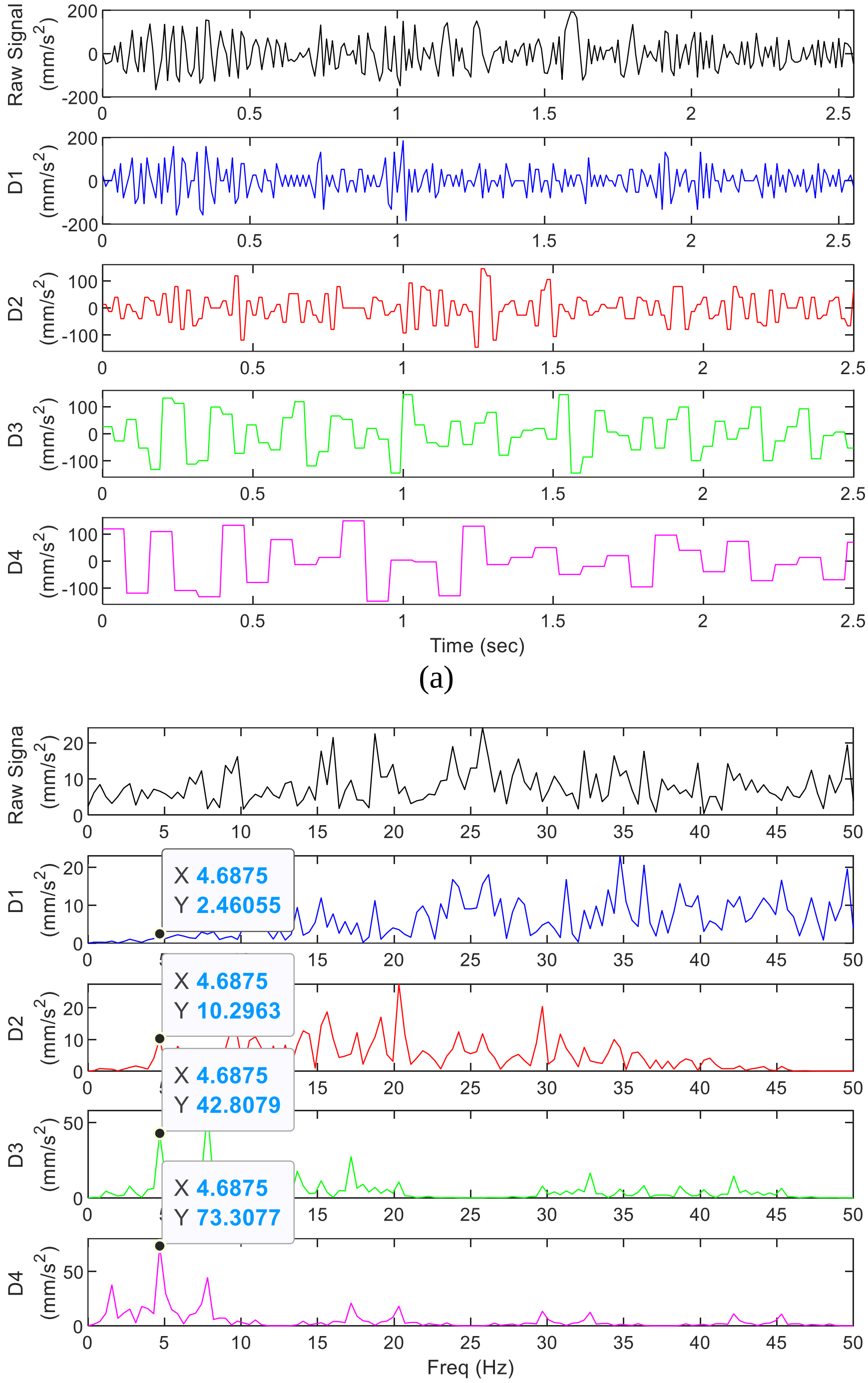

(a)

(b)

Figure 19. Signal decomposition in time and frequency domains for five-axles truck vehicle excitations

3.5. Comparison of the fundamental frequency amplitude of various types of vehicles.

Both EMD and WPD method exhibit a consistent pattern when it comes to analysing the impact of increasing vehicle weight on the bridge. As the weight of the vehicle passing through the bridge increases, there is an observable increase in the amplitude at the peak frequency 4.688 Hz. Table 2 presents a summary of the EMD and WPD combined with FFT result at a frequency of 4.688 Hz for various types of vehicles, including bus, two-axle truck, three-axle truck, four-axle truck, and five-axle truck. The results show that as the weight of the vehicle increases, the amplitude of vibrations produced on the bridge also increases. For example, the vehicle type I a bus generates an amplitude of about 19.2 mm/s², the vehicle type V while a five-axle truck produces the highest amplitude, reaching 91.0 mm/s². EMD typically captures larger amplitudes compared to WPD, providing a more sensitive indication of the bridge's response. According to Table 2, the maximum amplitude increases when the type of vehicle increases which is related to the total weight of the vehicle.These findings are important for monitoring bridge health, as identifying the impacts of heavy vehicles can aid in maintenance planning.

An increasing pattern on the vibration amplitude as the vehicle weight increases is also presented in Figure 20. Figure 20 shows the plot of the IMF2 of EMD method and D4 of the WPD method. Therefore, the main external factors influencing the vibration of the bridge are the vehicle's weight and the number of axles. This highlights that any ground movement caused by heavy vehicles or other dynamic factors can significantly impact the structural condition of the bridge. Consequently, the data recorded by the installed Bridge Health Monitoring System (BHMS) on all large-scale bridges is vital and will have a crucial influence on the socio-economic well-being of the surrounding communities.

Table 2. Maximum amplitude of fundamental frequency of 4.688 Hz for both EMD and WPD method.

Vehicle Type	Max. Amplitude (mm/s^2)	
Signal Processing Technique	EMD	WPD
IMF/Decomposition Element	IMF2	D4
Type I (Bus)	19.202	9.471
Type II (Two-axles truck)	33.074	21.037
Type III (Three-axles truck)	64.736	38.823
Type IV (Four-axles truck)	76.202	69.931
Type V (Five-axles truck)	91.001	73.308

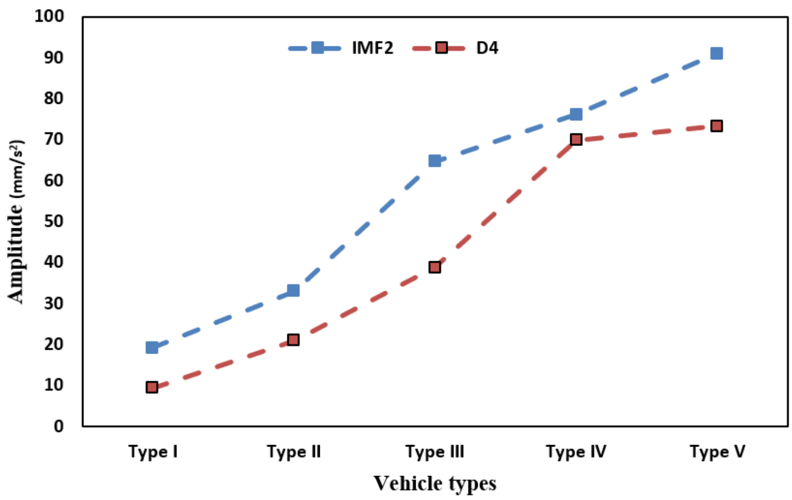

Figure 20. Amplitude of IMF2 and D4 at 4.688 Hz for five types of vehicles.

4. Conclusions

This research highlights the importance of structural health monitoring for bridges, particularly in countries undertaking large-scale infrastructure projects. By integrating advanced signal processing techniques with the Finite Element Method (FEM), the study offers a more efficient and cost-effective approach to maintaining and extending the lifespan of bridge structures. A key contribution of this research is the validation of using a reduced number of sensors to collect vibration data, significantly lowering both the cost and complexity of the monitoring system. The results demonstrate that vibration data generated by vehicles crossing the bridge can be effectively processed using EMD and WPD, in combination with FFT, to extract meaningful insights into structural conditions. In this study, the WPD method outperformed EMD in terms of accuracy and sensitivity. The findings also indicate a direct correlation between vehicle weight and increased vibration amplitude—an important indicator of structural integrity. Moreover, the successful preliminary tests conducted on the Cisomang Bridge validate the feasibility of applying FEM and vibration analysis for real-world bridge health monitoring. Continuous advancements in monitoring technology are expected to enhance the global safety and reliability of bridges. This research underscores the importance of integrating field data with computational modeling to achieve more accurate and practical monitoring solutions.

Acknowledgments

This research was supported by RIIM Kompetisi funding from the Indonesia Endowment Fund for Education (LPDP), Ministry of Finance of the Republic of Indonesia, and the National Research and Innovation Agency (BRIN), under contract number: 81/IV/KS/05/2023.

Author Contribution

Conceptualization: Seno Adi Putra, Muhammad Nazri, Yogi Reza Ramadhan; Methodology: Muhammad Nazri**,** Natalino Fonseca D. S. Guterres, Salustiano dos Reis Piedade; Data Collection: Yogi Reza Ramadhan, Seno Adi Putra, Marina Riviani Rompas; Data Analysis: Yogi Reza Ramadhan, Muhammad Nazri, Januar Panca Adi; Writing: Yogi Reza Ramadhan, Januar Panca Adi, Natalino Fonseca D. S. Guterres; Supervision: Seno Adi Putra, Yogi Reza Ramadhan; Funding: Seno Adi Putra.

Competing Interest

The financial support of this study has infomed in the acknowledge and the all authors declared that there is no personal, or professional relationships that might influence or appear to influence their research.

References

[1] Gastineau, A.; Johnson, T.; Schultz, A. (2009). Bridge health monitoring and inspections systems – A survey of methods. Department of Transportation, St. Paul, Minnesota, *USA*, Report No. MN/RC 2009-29.

[2] State of the practice and art for structural health monitoring of bridge. (accessed on 13 April 2022) Available online: https://www.fhwa.dot.gov/publications/research/infrastructure/structures/bridge/09040/09040.pdf

[3] Zhu, Y.; Liu, C.; Zhang, J. (2025). Identification of bridge modal parameter based on tire pressure monitoring of two-axle vehicle. *Journal of Sound and Vibration*, *606*, 119020. https://doi.org/10.1016/j.jsv.2025.119020.

[4] Huang, N.E.; Shen, Z.; Long, S.R.; Wu, M.C.; Shih, H.H.; Zheng, Q.; Yen, N.C.; Tung, C.C.; Liu, H.H. (1998). The empirical mode decomposition and the Hilbert spectrum for nonlinear and non-stationary time series analysis. *Proceedings of the Royal Society of London A*, *454*, 903–995. https://doi.org/10.1098/rspa.1998.0193.

[5] Braun, S.; Feldman, M. (2011). Decomposition of non-stationary signals into varying time scales: Some aspects of the EMD and HVD methods. *Mechanical Systems and Signal Processing*, *25*, 2608–2630. https://doi.org/10.1016/j.ymssp.2011.01.014.

[6] Caesarendra, W.; Kosasih, B.; Tieu, A.K.; Moodie, C.A.S. (2014). Circular domain features based condition monitoring for low speed slewing bearing. *Mechanical Systems and Signal Processing*, *45*, 114–138. https://doi.org/10.1016/j.ymssp.2013.12.002.

[7] Caesarendra, W.; Kosasih, P.B.; Tieu, A.K.; Moodie, C.A.S.; Choi, B.K. (2013). Condition monitoring of naturally damaged slow speed slewing bearing based on ensemble empirical mode decomposition. *Journal of Mechanical Science and Technology*, *27*, 1–10. https://doi.org/10.1007/s12206-012-1251-4.

[8] Chen, J. (2009). Application of empirical mode decomposition in structural health monitoring: Some experience. *Advances in Adaptive Data Analysis*, *1*, 601–621. https://doi.org/10.1142/S1793536909000275.

[9] O'Brien, E.J.; Malekjafarian, A.; González, A. (2019). Application of empirical mode decomposition to drive-by bridge damage detection. *European Journal of Mechanics - A/Solids*, *61*, 151–163. https://doi.org/10.1016/j.euromechsol.2016.10.007.

[10] Aied, H.; González, A.; Cantero, D. (2016). Identification of sudden stiffness changes in the acceleration response of a bridge to moving loads using ensemble empirical mode decomposition. *Mechanical Systems and Signal Processing*, *66–67*, 314–338. https://doi.org/10.1016/j.ymssp.2015.03.010.

[11] Zhu, L.; Malekjafarian, A. (2019). On the use of ensemble empirical mode decomposition for the identification of bridge frequency from the responses measured in a passing vehicle. *Infrastructures*, *4*, 32. https://doi.org/10.3390/infrastructures4030032.

[12] Press Release PT JASA MARGA (Persero) Tbk, No. 122/2019, 10 Juni 2019. (accessed on 13 April 2022) Available online: https://www.jasamarga.com/public/id/aktivitas/detail.aspx.

[13] Wang, S.; Huang, W.; Zhu, Z.K. (2011). Transient modeling and parameter identification based on wavelet and correlation filtering for rotating machine fault diagnosis. *Mechanical Systems and Signal Processing*, *25*, 1299–1320. https://doi.org/10.1016/j.ymssp.2010.10.013.

[14] Widodo, A.; Yang, B.S. (2008). Wavelet support vector machine for induction machine fault diagnosis based on transient current signal. *Expert Systems with Applications*, *35*, 307–316. https://doi.org/10.1016/j.eswa.2007.06.018.

[15] Daubechies, I. (1992). Ten Lectures on Wavelet. Society for Industrial and Applied Mathematics (SIAM), Pennsylvania, USA. https://doi.org/10.1137/1.9781611970104.